Functional Materials 13, No.1 (2006) © 2006 — Institute for Single Crystals

Optical properties of the modified structures of surface layers of amorphous metallic alloy ribbons

L.V.Poperenko, V.G.Kravets, S.I.Lysenko[*], *K.L.Vinnichenko*

T.Shevchenko Kyiv National University,
64 Volodymyrska St., 01033 Kyiv, Ukraine
[*]V.Lashkaryov Institute of Semiconductor Physics,
National Academy of Sciences of Ukraine,
41 Nauki Ave., 03028 Kyiv, Ukraine

Modification of the microrelief and structure of a Co-based amorphous metal alloy ribbon surface layers after thermal treatment at elevated and cryogenic temperatures and under an external magnetic field has been studied using light scattering method and atomic force microscopy. The surface roughness parameters were calculated from the experimental light scattering indicatrices. It is shown that heating of the metal ribbons to T = 350–475°C relieves partially the stresses arising in the course of the ribbon preparation and increases the surface roughness as compared to that of as-prepared samples.

Модификация микрорельефа и структуры поверхностных слоев лент аморфных сплавов на основе Co после термической обработки при повышенных и криогенных температурах, под действием приложенного магнитного поля изучена методом рассеяния света и атомно-силовой микроскопией. Параметры шероховатости поверхности лент рассчитаны из экспериментально полученных индикатрис интенсивности рассеянного света. Показано, что нагревание металлических лент до T = 350–475°C частично снимает напряжения, возникающие во время изготовления ленты, и повышает шероховатость поверхности по сравнению с той, которая характерна для свежеизготовленных образцов.

Cobalt-based amorphous metallic alloys (AMAs) are under intense study in view of their wide practical application as recording media. The magnetic and electronic properties of such materials prepared as ribbons formed by the melt spinning differ significantly from the properties of corresponding crystalline analogues. The differences are defined not only by the structure formed in the course of the material preparation but also by subsequent thermal and cryogenic treatments. When amorphous metal alloys are thermally treated, external fields or stresses also change the surface relief, which is related to the surface diffusion and structural phase transformations in the surface layer. Such processes are accompanied by migration of both individual atoms and aggregates thereof (including hundreds and thousands of atoms) to the surface [1]. In this case, the surface re-building occurs mainly at the nano- and microlevels, since much lower energy is required to change the size, shape, and location of microscopic irregularities as compared to macroscopic surface irregularities. It is to note that in most studies of amorphous metallic alloys, the main attention was given to the atomic structure. At the same time, the surface-layer microrelief modifications due to heat treatment remain unstudied in many aspects. The highly informative method of light scattering was used to study the surface layer microrelief and elastically strained state of amorphous alloy ribbons. It is well known that the spatial distribution and polarization characteristics of scattered light are completely defined by the

surface state [2]. The investigation of the scattered light field provides information on the optical properties and statistical distribution of surface inhomogeneities within relatively large areas (thousands of square micrometers).

The light scattering from a surface characterized by low root-mean square roughness (much less than the wavelength of the probing light) is linear. The light scattered from individual relief components can be singled out of the scattered light spatial distribution and analyzed independently. For that analysis, the surface relief is represented in the form of a two-dimensional sum of diffraction gratings with different periods, amplitudes, and phases [2]. The scattering from one diffraction grating with a fixed spatial frequency (the inverse period of the grating) occurs in a certain angular range. Hence, the light scattering method provides information on the set of such gratings. In this case, it is convenient to represent and analyze the scattering data according to the spatial frequency value in the expansion of the surface relief f that is related to the polar scattering angle θ by the expression $f = \sin\theta/\lambda$. The experimental light scattering data for a low roughness surface can be used to calculate the power spectral density (PSD) functions for the surface roughness. The PSD function yields information on the statistical distribution and size of surface asperities with different spatial frequencies; it is equal to the squared magnitude of the Fourier transform of the function $h(\rho)$, which describes the surface microrelief:

$$PSD(\mathbf{f}) = \left| \int_{-\infty}^{\infty} h(\boldsymbol{\rho}) e^{i(\mathbf{f}\boldsymbol{\rho})} d\boldsymbol{\rho} \right|^2,$$

where ρ is the radius vector extending from the origin of coordinates to a point in the surface.

For investigations, ribbons of the amorphous metal alloy $Co_{59}Fe_5Ni_{10}Si_{11}B_{15}$ were prepared using the melt spinning method [3]. There were two series of the samples. The first one consisted of the samples annealed at T_a = 350, 400, 425, and 475°C for 10 min, while the second one included the samples subjected to cryogenic treatment at liquid nitrogen temperature (T = 78 K) for four hours followed by heating up to room temperature or to the cryogenic treatment in a magnetic field (B ~ 30 mT) directed perpendicularly to the ribbon surface as well as to the laser treatment

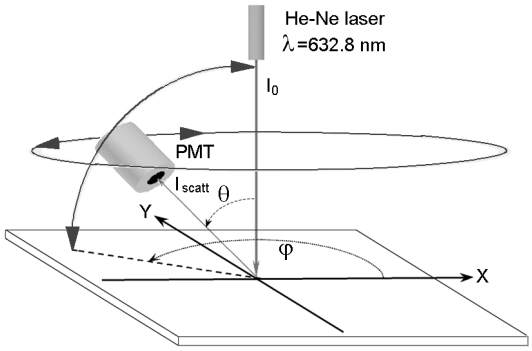

Fig. 1. Scheme of experimental setup to measure angular distribution of light scattering intensity.

(λ = 1064 nm). The cryogenic treatment was performed as follows. The amorphous alloy samples were immersed for 4 h in a Dewar flask with liquid nitrogen and then heated to room temperature in air.

The microrelief of the amorphous alloy ribbons was studied by analyzing the spatial intensity distribution of the light scattered from the surface under study. The circularly polarized light with the intensity I_0 generated by the He–Ne laser (the wavelength λ = 632.8 nm) was incident normally on the sample surface (Fig. 1). Such a polarization was chosen to exclude the contribution of scattering anisotropy associated with the polarization effects. The light spot diameter did not exceed 100 μm. The scattered light (intensity I_{scat}) was detected by a photomultiplier rotated with respect to the point of measurement in the azimuthal and polar directions using stepper motors. Such a variation of the photomultiplier angular position made it possible to measure the scattered light distribution within the hemisphere above the sample surface. Along with measurements of the light scattering within the hemisphere, we also analyzed the polar dependences of the scattered light intensity at a fixed azimuthal angle φ. Such measurements were performed for several surface areas located close to the axial line of a ribbon, then the scattering data for different areas were averaged. The light scattering data were used to calculate the scattered light normalized intensity ARS (angle-resolved scattering) as a function of the angles θ and φ by the relation [2]

$$ARS(\theta,\varphi) = \frac{1}{I_0}\left(\frac{dI_{scatt}(\theta,\varphi)}{d\Omega}\right),$$

where dI_{scatt} is the intensity of light scattered within the solid angle $d\Omega$.

The surface microrelief of amorphous alloy ribbons as-cast and thermally annealed at T_a = 350, 400, 425 and 475°C for 10 min was investigated by AFM, too. The study was carried out using a TopoMetrix SPM Atomic Force Microscope. The experiments were fulfilled using contact regime in air. The 10×10 μm^2 areas of ribbon surface were studied. The roughness parameters R_q, R_a, R_z and R_m were determined for surfaces of these ribbons. These parameters were calculated by means of TopoMetrix SPMLab programme. After mathematical data processing, the quantitative characteristics of roughness were obtained. Among those, the most widely-used one is the root-mean square surface roughness height [4]:

$$R_q = \frac{1}{n}\sum_{i=1}^{n} \sqrt{(z_i - \bar{z})^2} \ ,$$

where $\bar{z}$ is average profile (the mean plane) of the surface as well as average (arithmetic) roughness parameter R_a which is a measure of the absolute deviation of the profile ordinate heights Z_i from the mean (reference) plane:

$$R_a = \frac{1}{n}\sum_{i=1}^{n} \left| z_i - \bar{z} \right| .$$

The value R_z as a difference between heights of the highest and lowest points of the surface or peak-to-valley roughness height and the value R_m as a maximal height of the surface have been incorporated into often measured magnitude.

The surface under study contains asperity of two types. There are (1) macroscopic irregularities of heights comparable to the probing light wavelength and characteristic dimensions in the lateral direction of a few tens of micrometers and (2) micro-irregularities of heights much lower than the radiation wavelength. The macroscopic asperity arises upon preparation of the amorphous alloy samples due to the melt spreading over the rotating disk and the subsequent fast quenching [5]. Due to this specific features of the sample preparation, the macroscopic asperity had the shape of linear depressions oriented along the direction of the melt spreading. The characteristic size of the micro-irregularities is several tens

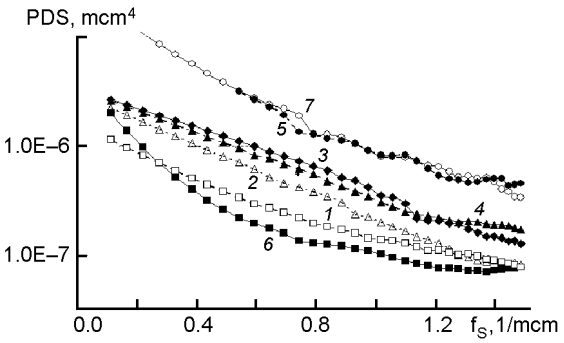

Fig. 2. PSD functions calculated for amorphous $Co_{59}Fe_5Ni_{10}Si_{11}B_{15}$ alloy samples as-cast (*1*) and annealed at T_a (°C): 350 (*2*), 375 (*3*), 400 (*4*), 425 (*5*), 450 (*6*) and 475 (*7*).

times smaller, and those are located within the macroscopic irregularities.

Since the surface macroscopic irregularities are oriented along the longitudinal axis of the amorphous alloy ribbon, the light scattered from those shows an anisotropy with a maximum in the indicatrix at the azimuthal angle φ = 90°. The scattering occurs within the range of polar angles θ from 0° to 12°, which correspond to low spatial frequencies (from 0 to 0.4 μm^{-1}), and exceeds the scattering from micro-irregularities by several orders of magnitude. As a result, a significant change in the scattering intensity is observed in the vicinity of the polar angle θ = 12°, which made it difficult to measure the scattered light within the entire hemisphere. Since the processes of surface re-building caused by thermal treatments and the action of external fields occur mainly at the nano- and microlevels, it was of interest to study the height parameters of the surface microrelief, i.e., the micro-irregularities characterized by high spatial frequencies. Therefore, in this study, we have analyzed the scattered light field in the range of polar angles from 12° to 90° where no scattering from the macroscopic surface irregularities is observed. The indicatrices of the normalized scattering intensity ARS (θ, φ) for amorphous alloy $Co_{59}Fe_5Ni_{10}Si_{11}B_{15}$ ribbon have been obtained. The azimuthal distribution ARS(θ, φ) is described by closed curves (isophotes) indicating the equal intensity levels of the scattered light. For a surface of this as-cast ribbon that was not thermally treated, any optical anisotropy was not observed . Moreover, despite of results on Fe-based amorphous alloys [6], for the investigated Co-based ones after both cryogenic treatment

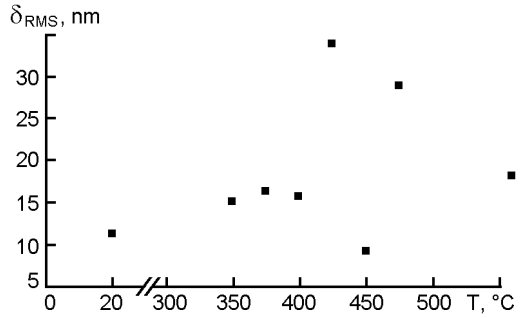

Fig. 3. Dependence of root-mean square roughness parameter on the annealing temperature for non-contact ribbon surfaces of amorphous $Co_{59}Fe_5Ni_{10}Si_{11}B_{15}$ alloy in accordance with light scattering data.

without and with applied magnetic field as well as laser annealing after the mentioned treatment, the optical anisotropy was not found, too. In our opinion, this result for Co-based amorphous alloy may be related to zero magnetostriction of such alloy and its weak temperature dependence.

When considering the light scattering measurement data expressed as PSD dependences (Fig. 2), the appropriate curves are seen to have the same slope for as-cast samples (at several probing areas by the mentioned optical method) and those annealed at temperatures up to 425°C. This means that the ribbon surfaces are homogeneous and possess isotropic optical properties. But after annealing of the ribbons at 450°C, some small changes in low spatial frequency range due to enhancement of the PSD curve slope are observed. This is connected with a slight surface layer structure modification and changes in the statistical distribution character of the macroscopic irregularities. Similar behavior of the PSD curve is also observed at $T = 475$°C. The measurement of the light scattering intensity as a function of θ (φ = const) as corresponding PSD function yields the roughness parameters which can be calculated basing thereon. The obtained values of the roughness parameters are presented in Fig. 3, and then were confirmed by atomic force microscopy data.

Figs. 4a–4d, present the 3D-images of the non-contact side surface of a ribbon of amorphous metallic alloy $Co_{59}Fe_5Ni_{10}Si_{11}B_{15}$ as-cast and subjected to isochronic thermal annealing. At vertical axis, the parameter R_m which corresponds to maximal height of the surface microrelief roughness is presented. It is to note that along ordinate axis

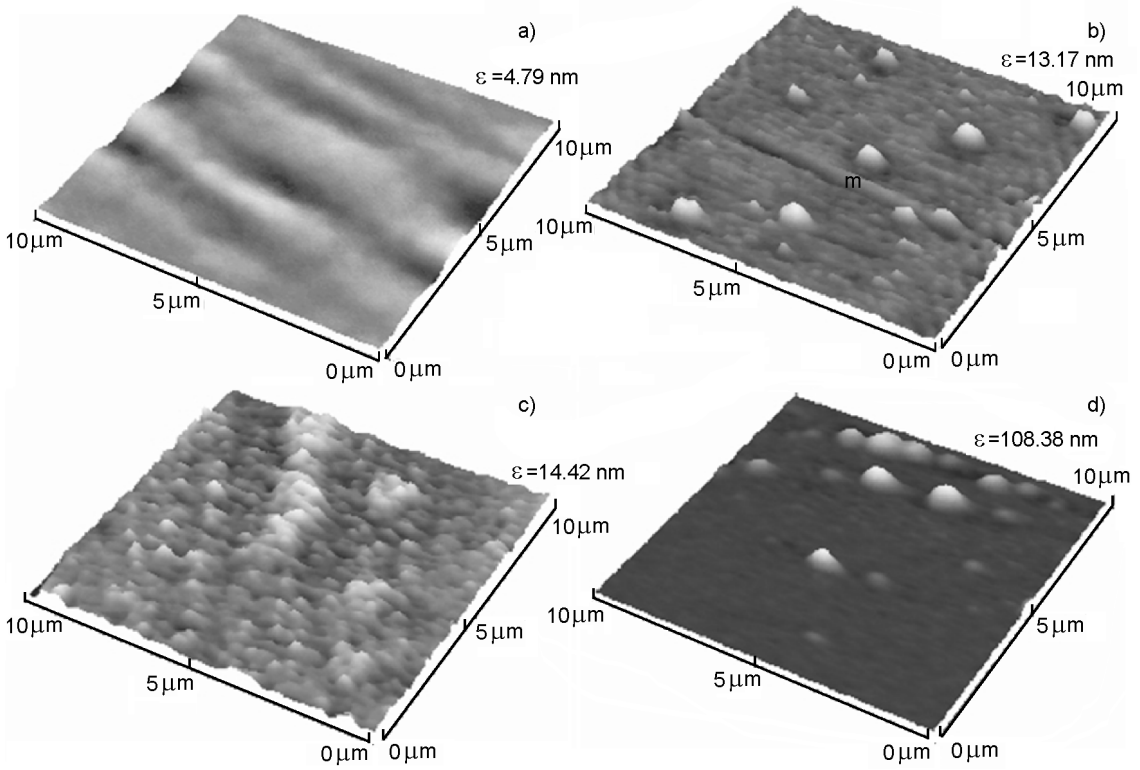

Fig. 4. Atomic force microscopy data for a 10×10 μm^2 area at the non-contact surface of as-cast (a), and thermally annealed at T (°C): 350 (b), 425 (c) and 475 (d) amorphous $Co_{59}Fe_5Ni_{10}Si_{11}B_{15}$ alloy sample.

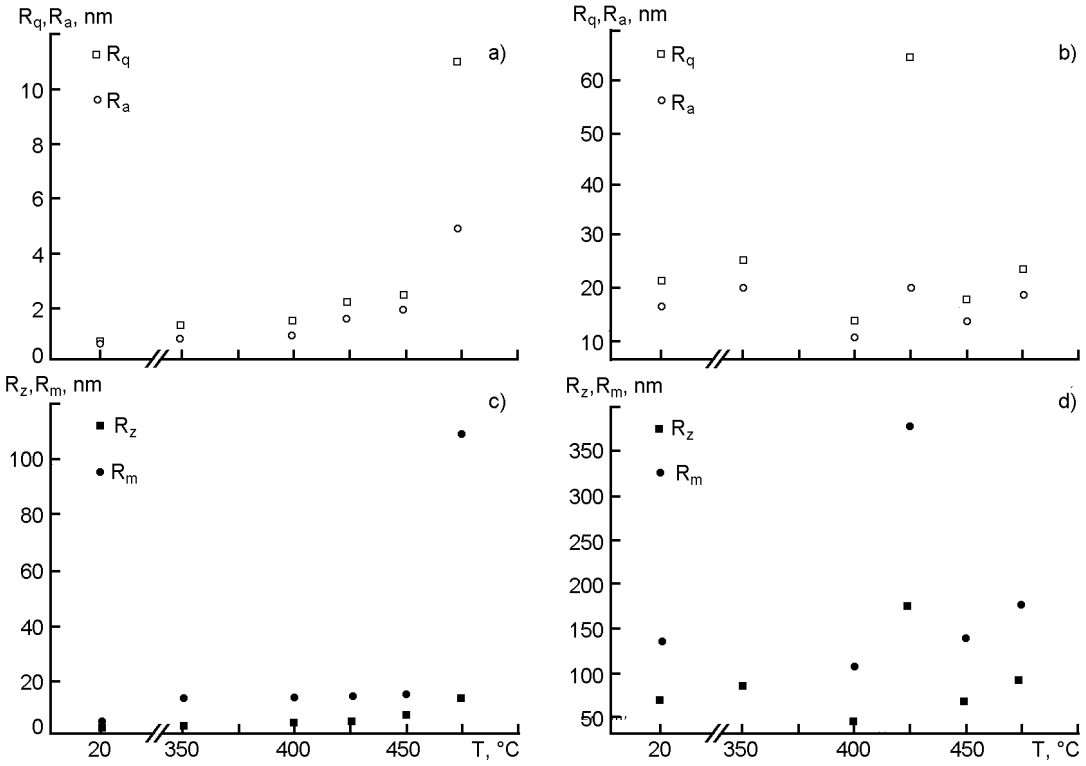

Fig. 5. Dependences of roughness parameters R_q, R_a (a,b) and R_z, R_m (c,d) on annealing temperature for non-contact (a and c) and contact (b,d) ribbon surfaces of amorphous $Co_{59}Fe_5Ni_{10}Si_{11}B_{15}$ alloy in accordance with AFM data.

in Fig. 4d, a smaller scale is selected to describe the appropriate surface roughness. It is seen from Fig. 4a that the noncontact surface of as-cast ribbon shows a rather smooth microrelief with periodic alternation of peaks and valleys at the maximal roughness of 4.8 nm. The occurrence of such surface microrelief must be explained by peculiarities of the melt spreading at its quenching during the ribbon preparation by spinning method. The annealing of a ribbon at T_a = 350°C (Fig. 4b) causes the appearance of microrelief features as peaks of about 10 nm height and lateral profile size of 1 μm or less on the surface that has the characteristics similar to those for as-cast ribbon. Thermal annealing at higher temperature T_a = 425°C (Fig. 4c) causes the appearance of smaller peaks of about the same height as at T_a = 350°C. As a result, the number of such peaks on the area investigated increases considerably. Thermal annealing at the highest temperature T_a = 475°C (Fig. 4d) results in isolated peaks of more than 100 nm height with lateral dimensions of about 1 μm. Such changes of the amorphous ribbon surface morphology under thermal annealing agree with the results obtained by scanning tunneling microscopy in [7] for binary metal-metalloid amorphous system.

As to the microrelief of as-cast Co-based amorphous ribbon surface that was in contact with disk-cooler during quenching, isolated valleys and peaks of larger than 100 nm height and lateral dimensions of several micrometers are characteristic. Such peculiarities could be explained by air capture during melt quenching resulting in formation of bubbles at the disk-cooler/ribbon interface. At the non-contact surface of as-cast sample, no similar features are present. The annealing at elevated temperatures causes a gradual enhancement of the roughness parameter for control surface without essential evolution of the surface microrelief (T_a = 350 and 475°C) as compared to data for as-cast ribbon. The only except is the ribbon annealed at T_a = 425°C where the peaks higher than 300 nm with lateral dimensions of several micrometers are observed.

The dependences of ribbon surface roughness parameters on the annealing temperature for non-contact and contact ribbon surfaces are shown in Fig. 5. It is seen that roughness parameters R_q and R_a of non-contact ribbon surface (Fig. 5a) rise monoto-

nously from R_q = 0.7 nm, R_a = 0.5 nm for as-cast rapidly quenched sample (T = 20°C) to R_q = 1.3–2.4 nm, R_a = 0.9–1.8 nm for the ribbon surface annealed at T_a = 350–450°C. As the annealing temperature rises up to T_a = 475°C, an appreciable increase of both root mean square (R_q) and average (R_a) surface roughness parameters is observed and these parameters become R_q = 11 nm and R_a = 4.9 nm, respectively. The parameter R_z for non-contact ribbon surface (Fig. 5c) increases monotonously from 2.3 nm for as-cast sample to 14 nm for the sample annealed at the highest temperature T_a = 475°C. Similar changes are typical of the parameter R_m but for the sample annealed at 475°C, this parameter increases up to 109 nm.

The obtained microrelief evolution for non-contact surface at thermal annealing and the dependence of roughness parameters on annealing temperature evidence the initiating crystallization of the Co-based amorphous alloy at the highest annealing temperature, because for alloy being studied, the crystallization temperature T_{cr} in accordance with X-ray analysis data is 492°C. It is beyond doubt that the monotonous rise of the non-contact surface roughness parameters at increasing annealing temperature is due to structural relaxation of the Co-based amorphous alloy. The relaxation process of such type takes place in the temperature interval T_a = 350–475°C. It is of importance that the microrelief evolution obtained after pre-crystallization annealing for amorphous alloy $Co_{59}Fe_5Ni_{10}Si_{11}B_{15}$ corresponds to the crystallization onset of the ribbon beginning from its surface. Similar changes, namely the crystallization onset in amorphous ribbon within its surface layer with conservation of amorphous structure in the bulk was observed in [8] for amorphous alloy $Fe_{80}B_{20}$.

For the contact surface (Fig. 5b and 5d) of as-cast Co-based amorphous alloy, the roughness parameter values exceed by more than one order their values for non-contact surface. The characteristic difference in temperature dependence of the roughness parameters for contact surface consists in that all the determined parameters increase during annealing at T_a = 350°C, their further decrease at T_a = 400°C and show a sharp jump at T_a = 425°C. Only the parameter R_a does not show such sharp changes. Thus, the roughness parameters for contact ribbon surface change more chaotically under thermal annealing than those of the non-contact surface.

Thus, using the atomic force microscopy, it has been shown that thermal annealing of amorphous alloy results in monotonous rise of the roughness parameters for the ribbon non-contact surface. The changes may be explained by the incipient crystallization process at the highest annealing temperature. For the ribbon contact surface, the roughness parameters show oscillations with maximal increase at T_a = 425°C. The spectral magneto-optical research has been also carried out for such Co-based amorphous alloys. The experimental values of polar Kerr rotation θ_p and ellipticity η_p for Co-based ribbons in the incident photon energy range $0.6 \le h\omega \le 2.2$ eV have been determined. Our results are in good agreement with data of magneto-optical study of similar Co-based alloy system [9] which has shown a high density of hcp Co grains in the annealed ribbon film.

References

1. B.A.Nesterenko, V.G.Lyapin, in: Phase Transitions on Free Faces and Interphase Boundaries in Semiconductors, Naukova Dumka, Kiev (1990) [in Russian].
2. J.M.Bennett, L.Mattson, in: Introduction to Surface Roughness and Scattering, Opt. Soc. Amer., Washington, D.C. (1989).
3. H.Liberman, in: Amorphous Metal Alloys, ed. by F.E.Lyuborskiy, Metallurgiya, Moscow (1987), p.38 [in Russian].
4. G.Binnig, C.F.Quate, Ch.Gerber, *Phys. Rev. Lett.*, **56**, 930 (1986).
5. L.V.Poperenko, V.G.Kravets, *Optika i Spektr.*, **86**, 621 (1999).
6. L.V.Poperenko, S.I.Lysenko, K.L.Vinnichenko, *Optika i Spektr.*, **96**, 292 (2004).
7. D.E.Burgler, C.M.Schmidt, D.M. Schaller et al., *Phys. Rev. B*, **59**, 10895 (1999).
8. P.Vavassori, F.Ronconi, E.Puppin, *J. Appl. Phys.*, **82**, 6177 (1997).
9. V.Kravets, A.Petford-Long, X.Portier, L.Poperenko., *Materials Science Forum*, **373–376**, 481 (2001).

Оптичні властивості модифікованих структур поверхневих шарів стрічок аморфного металевого сплава

Л.В.Поперенко, В.Г.Кравець, С.І.Лисенко, К.Л.Вінніченко

Модифікація мікрорельєфа і структури поверхневих шарів стрічок аморфних сплавів на основі Co після термічної обробки при підвищених та кріогенних температурах, під дією прикладеного магнітного поля вивчена методом розсіяння світла і атомно-силовою мікроскопією. Параметри шорсткості поверхні розраховано із експериментально отриманих індикатрис інтенсивності розсіяння світла. Показано, що нагрівання металевих стрічок до $T = 350–475$°C частково знімає напруження, що виникає під час виготовлення стрічки, і підвищує шорсткість поверхні порівняно з тією, яка характерна для щойно виготовлених зразків.